JCAMECH

Vol. 49, No. 2, December 2018, pp 395-407
DOI: 10.22059/jcamech.2018.261764.300

Magneto-Thermo mechanical vibration analysis of FG nanoplate embedded on Visco Pasternak foundation

Abbas Moradi[a],*, Amin Yaghootian[a], Mehdi Jalalvand[b], Afshin Ghanbarzadeh[a]

[a] Department of Mechanical Engineering, Shahid Chamran University of Ahvaz, Ahvaz, Iran

[b] Department of Mathematics and Computer Science, Shahid Chamran University of Ahvaz, Ahvaz, Iran

ARTICLE INFO

Article history:
Received: 12 July 2018
Accepted: 1 September 2018
Available online

Keywords:
Circular and annular nanoplate
Magnet field
Functional graded nanoplate
Modified strain gradient theory
Modified couple stress theory

ABSTRACT

In this paper, the mechanical vibration analysis of functionally graded (FG) nanoplate embedded in visco Pasternak foundation incorporating magnet and thermal effects is investigated. It is supposed that a uniform radial magnetic field acts on the top surface of the plate and the magnetic permeability coefficient of the plate along its thickness are assumed to vary according to the volume distribution function. The effect of in-plane pre-load, viscoelastic foundation, magnetic field and temperature change is studied on the vibration frequencies of functionally graded annular and circular nanoplate. Two different size dependent theories also are employed to obtain the vibration frequencies of the FG circular and annular nanoplate. It is assumed that a power-law model is adopted to describe the variation of functionally graded (FG) material properties. The FG circular and annular nanoplate is coupled by an enclosing viscoelastic medium which is simulated as a visco Pasternak foundation. The governing equation is derived for FG circular and annular nanoplate using the modified strain gradient theory (MSGT) and the modified couple stress theory (MCST). The differential quadrature method (DQM) and the Galerkin method (GM) are utilized to solve the governing equation to obtain the frequency vibration of FG circular and annular nanoplate. Subsequently, the results are compared with valid results reported in the literature. The effects of the size dependent, the in-plane pre-load, the temperature change, the magnetic field, the power index parameter, the elastic medium and the boundary conditions on the natural frequencies are scrutinized. According to the results, the application of radial magnetic field to the top surface of plate gives rise to change the state of stresses in both tangential and radial direction as well as the natural frequency. Also, The temperature changes play significant role in the mechanical analysis of FG annular and circular nanoplate. This study can be useful to product the sensors and devices at the nanoscale with considering the thermally and magnetically vibration properties of the nanoplate

1. Introduction

Functionally graded materials (FGMs) are inhomogeneous composites that can be described as the gradually variation of material microstructure from one material to another material. FGMs have recently attracted much attention due to its merits including improved stress distribution, higher fracture toughness and reduced stress intensity factors, enhanced the thermal resistance. With the development of advance material science and technology, FGMs have been utilized in various engineering fields such as micro/Nano electro mechanical systems, thin films in the form of shape memory, alloys biomedical materials, and atomic force microscopy (AFM), space vehicles, reactor vessels, semiconductor industry and general structural elements in high thermal environments [1-9]. Therefore, considering static and dynamic behavior of functionally graded structures under different actuation is very significant.

As experiments on nanoscale objects are often fraught with uncertainty due to the difficulty of fabricating and manipulating these objects at length scales below ≈10 nm [10], size dependent continuum theories have been commonly used to simulate material discontinuities in micro/nano-scales. To predict the responses of nanostructures under different loading conditions, theoretical analysis have been more noteworthy because the experimental methods are encountered in difficulties when the size of physical systems is scaled down into the nanoscale. There are several size-dependent continuum theories such as couple stress

* Corresponding Author. *Email*: a.moradi64@gmail.com

theory(CST) [11], strain gradient elasticity theory(SGT), modified couple stress theory(MCST) [12] and nonlocal elasticity theory [13-16]. From among these theories, modified strain gradient theory (MSGT) is one of the most practical theoretical techniques for the studying of MEMS/NEMS devices due to their computational efficiency and accuracy compared with to the atomistic model ones. Numerous works have been conducted on the mechanical performance of functionally graded material structures, including buckling and dynamic stability, bending, free Vibration.

The linear free and forced vibration of FGM circular plates and annular sectorial plates was studied by Nie and Zhong [17] using the DQ method, respectively. The nonlinear vibration of functionally graded beams based on Euler-Bernoulli beam theory and von Kármán geometric nonlinearity was investigated by Ke et al. [18] using the direct numerical integration method and Runge-Kutta method. Xia and Shen [19] considered vibration analysis for compressively loaded and thermally loaded postbuckled FGM plates with piezoelectric fiber reinforced composite (PFRC) actuators based on a third order shear deformation plate theory and the general von Kármán-type equation. The free vibration of edge cracked cantilever microscale FGM beams was investigated by Akbaş [20] based on the modified couple stress theory (MCST). The free vibration of nanocomposite beams reinforced by single-walled carbon nanotubes was discussed by Lin and Xiang [21]. The free vibration analysis of radially FGM circular and annular sectorial thin plates of variable thickness, resting on the Pasternak elastic foundation was studied by Hosseini-Hashemi et al. [22]. Shamekhi and Nai [23] investigated the buckling analysis of radially-loaded circular FGM plate with variable thickness based on Love-Kichhoff hypothesis and the mesh-free method. The elastic solutions of an FGM disk with variable thickness subjected to a rotating load was provided by Bayat et al. [24]. The free vibration problem of sandwich FGM shell structures with variable thickness using the DQ method was considered by Tornabene et al. [25]. Wang et al. [26] studied Timoshenko Nano-beams formulations based on the modified strain gradient theory. Ansari et al. [27,28] analyzed the linear and nonlinear vibration characteristics of functionally graded microbeams based on SGT and Timoshenko beam theories. They illustrated that the value of material property gradient index plays a more important role in the vibrational response of the functionally graded microbeams with lower slenderness ratios. Recently, the free vibration response of functionally graded higher-order shear deformable microplates was investigated by Sahmani and Ansari [29] based on strain gradient elasticity theory. Ghayesh et al studied [30] the nonlinear forced vibrations of a microbeam employing strain gradient elasticity theory.

The buckling of rectangular nanoplate under shear in-plane load and thermal environment was analyzed by Mohammadi et al [31]. They found that the critical shear buckling load of rectangular nanoplate is strongly dependent on the small scale coefficient. Civalek and Akgoz [32] investigated the vibration behavior of micro-scaled sector shaped graphene surrounded by an elastic matrix. Employing the nonlocal elasticity theory to study the vibration of rectangular single layered graphene sheets (SLGSs) resting on an elastic foundation was considered by Murmu and Pradhan [33]. They have employed both Winkler-type and Pasternak-type models for simulate the interaction of the graphene sheets with a surrounding elastic foundation. The results showed that the natural frequencies of SLGSs are strongly dependent on the small scale coefficients. Pradhan and Phadikar [34] analyzed the vibration of multilayered graphene sheets (MLGS) based on nonlocal continuum models. They have shown that the nonlocal effect is quite significant and needs to be included in the continuum model of graphene sheet. Wang et al. [35] studied thermal effects on vibration properties of double-layered nanoplates at small scales. Reddy et al, [36] investigated the equilibrium configuration and continuum elastic properties of finite sized graphene. Aksencer and Aydogdu [37] proposed levy type solution for vibration and buckling of nanoplate. In this paper, they considered rectangular nanoplate with isotropic property without effect of elastic medium. Malekzadeh et al. [38] employed the differential quadrature method (DQM) to investigate the thermal buckling of a quadrilateral nanoplates resting on an elastic medium. Thermal vibration analysis of orthotropic nanoplates based on nonlocal continuum mechanics and two variable refined plate theory was considered by Satish et al. [39]. They represented vibration frequency of rectangular nanoplate just only for simply supported boundary conditions and they didn't represent vibration frequency for other boundary conditions. Prasanna Kumar et al. [40] studied thermal vibration analysis of monolayer graphene sheet with isotropic property embedded in an elastic medium via nonlocal continuum theory axisymmetric buckling of the circular graphene sheets with the nonlocal continuum plate model was represented by Farajpour et al. [41]. Moreover, they studied the buckling behavior of circular nanoplates under uniform radial compression. They showed that nonlocal effects play an important role in the buckling of circular nanoplates and the results predicted by nonlocal theory are in exactly match with MD results. The vibration analysis of circular and annular graphene sheet was studied by Mohammadi et al [42] using the nonlocal plate theory. The results revealed that the scale effect is less prominent in lower vibration mode numbers and is highly prominent in higher mode numbers.

The magneto-thermo-mechanical response of a FGM annular rotating disc with variable thickness was investigated by Bayat et al 43]. They observed that unlike the positive radial stresses developed in a mechanically loaded FGM disk, the radial stresses due to magneto-thermal load can be both tensile and compressive. Behravan Rad and Shariyat [44] studied a porous circular FG plate with variable thickness subjected to non-axisymmetric and non-uniform shear along with a normal traction and a magnetic actuation. The plate was supported on a non-uniform Kerr elastic foundation. They considered the effect of material, loading, boundary and elastic foundation on the resulting displacement, stress, Lorentz force, electromagnetic stress and magnetic perturbation quantities. Wang and Dai [45] derived analytical expressions for magneto dynamic stress and perturbation response of an axial magnetic field vector in an orthotropic cylinder under thermal and mechanical shock loads. They showed the response histories of dynamic stresses and the perturbation of the field vector. Nejad MZ, et al [46] investigated the buckling analysis of arbitrary two-directional functionally graded Euler-Bernoulli nano-beams based on nonlocal elasticity theory. The size dependent free vibration analysis of nanoplates made of functionally graded materials based on nonlocal elasticity theory with high order theories has been studied by Daneshmehr, Alireza et al [47]. Zargaripoora, A., et al [48] presented the free vibration analysis of nanoplates made of functionally graded materials based on nonlocal elasticity theory using finite element method. Nejad, Mohammad Zamani, et al [49] employed the Non-local analysis of free vibration of bi-directional functionally graded Euler-Bernoulli nano-beams. Hosseini, Mohammad, et al [50] proposed the stress analysis of rotating nano-disks of variable thickness made of functionally graded materials. Nejad, M.Z., et al [51] presented Eringen's non-local elasticity theory for bending analysis of bi-directional functionally graded Euler-Bernoulli nano-beams. Size-dependent stress analysis of single-wall carbon nanotube based on strain gradient theory has been proposed by

Hosseini, M., et al [52]. Zamani Nejad, Mohammad., et al [53] presented a review of functionally graded thick cylindrical and conical shells. Shishesaz, M., et al [54] investigated the analysis of FGM nanodisk under thermo elastic loading based on SGT. The vibration behavior of functional graded (FG) circular nanoplate embedded in a Visco-Pasternak foundation and coupled with temperature change is studied by Goodarzi et al [55].

It is obvious that the natural frequency is easily affected by the applied in-plane pre-load, magnetic field and temperature change. As a result, one of the practical interesting subjects is to study the effect of in-plane pre-load on the property of transverse vibration of functional graded circular and annular nanoplate. Researches that studied on the FG circular and annular nanoplate are very limited in number with respect to the case of rectangular nanoplate. Based on the available literature, this study tries to investigate the magneto-thermo elastic behavior of the FG circular and annular nanoplate embedded in a Visco-Pasternak elastic foundation based on the MCST. The governing equation of motion is deduced from Hamilton's principle. The DQM is utilized to solve the governing equations of FG circular and annular nanoplate with simply supported, clamped boundary conditions and the other boundary conditions. The results showed some new and absorbing phenomena, which are useful to design nano-electro-mechanical system and micro electro-mechanical systems devices using FG circular and annular nanoplate.

2. Fundamental Formulations

Consider a radial magnetic field vector $\vec{H}$ as shown in figure (1). The resulting Lorentz force f_z and the perturbation of electric field vector $\vec{e}$ acts along z and θ directions respectively. Now assume an annular circular plate with uniform transverse load P_0 acting on its top surface (see figure 2) is exposed to this magnetic field. As a result, the total transverse load acting on the plate, along z direction, would be, $q_z = P_0 + f_z$. This will induce a displacement field vector $\vec{U}$ in the plate.

Assuming the magnetic permeability $\mu(z)$ of the plate [46] is equal to the magnetic permeability of its surrounding, ignoring the displacement electric currents, the Maxwell's electrodynamics equations for the plate may be described as Wang X et al [45].

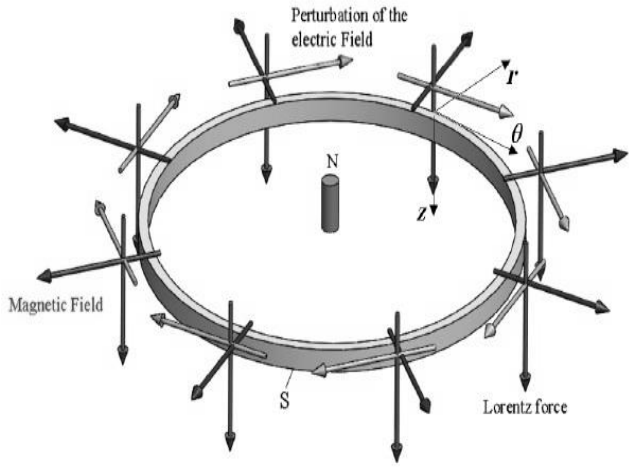

Fig 1. Radial magnetic field vector [9]

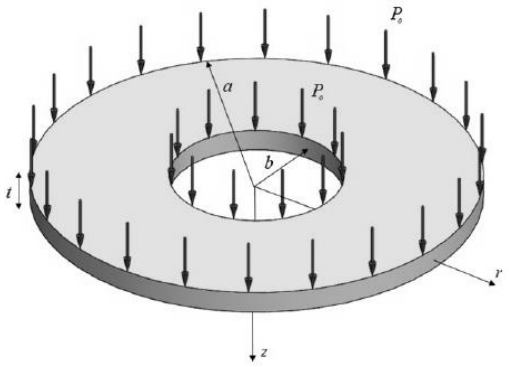

Fig 2. Geometry, loading and coordinate system of the annular plate [9]

$$\vec{j} = \vec{\nabla} \times \vec{h} \quad , \quad \vec{h} = \vec{\nabla} \times (\vec{U} \times \vec{H}) = curl(\vec{U} \times \vec{H}), \quad div\, \vec{h} = 0 \tag{1}$$

$$\vec{e} = -\mu(z)\left(\frac{\partial \vec{U}}{\partial t_0} \times \vec{H}\right) \quad , \quad \vec{\nabla} \times \vec{e} = -\mu(z)\frac{\partial \vec{h}}{\partial t_0} \tag{2}$$

Where $\vec{j}$ is the surface density vector of the electric current and $\vec{e}$ is the perturbation of the electric field vector, $\vec{h}$ is the perturbation of the magnetic field vector and t_0 is the time. Applying cylindrical coordinates (r,θ,z) application of the magnetic field vector $\vec{H}(H_r,0,0)$ to equations (1) and (2), results in:

$$\vec{U} = (u_r, 0, w) \quad , \quad \vec{h} = (0,0,h_z) \tag{3}$$

$$\vec{e} = -\mu(z)\left(0,0,H_r\frac{\partial}{\partial T}\left(\frac{\partial w}{\partial r} + \frac{w}{r}\right)\right) \tag{4}$$

$$\vec{j} = \left(0, -H_r\frac{\partial}{\partial r}\left(\frac{\partial w}{\partial r} + \frac{w}{r}\right), 0\right) \tag{5}$$

$$\vec{f}_z = \mu(z)(\vec{j} \times \vec{H}) = \mu(z)\, H_r{}^2\frac{\partial}{\partial T}\left(\frac{\partial w}{\partial r} + \frac{w}{r}\right) \tag{6}$$

$$\vec{h}_z = H_r\left(\frac{\partial w}{\partial r} + \frac{w}{r}\right) \tag{7}$$

3. Differential equations for nanoplate

A mono-layered circular and annular nanoplate resting on a Visco-Pasternak medium is shown in Fig.3, in which the geometrical parameters of outer radius, inner radius and thickness are also indicated by a, b and h respectively. In the present study, functionally graded materials made of metals and ceramics are studied. The bottom of the plate is assumed to be fully metallic while the top of the plate is fully ceramic. The variation of young's modulus, Poisson's ratio and density is assumed to vary by power law. The variations in the material properties are expressed as

$$E(z) = E_m + (E_c - E_m)\left(\frac{2z+h}{2h}\right)^k$$

$$\alpha(z) = \alpha_m + (\alpha_c - \alpha_m)\left(\frac{2z+h}{2h}\right)^k \qquad -\frac{h}{2} \le z \le \frac{h}{2}$$

$$\upsilon(z) = \upsilon_m + (\upsilon_c - \upsilon_m)\left(\frac{2z+h}{2h}\right)^k$$

$$\mu(z) = \mu_m + (\mu_c - \mu_m)\left(\frac{2z+h}{2h}\right)^k \tag{8}$$

Where, $E(z)$, $\alpha(z)$ and $\upsilon(z)$ are the Young's module, the thermal expansion and the Poisson's ratio respectively. To study the mechanical behavior of FG annular and circular nanoplate in thermal environment and magnet field, the Kirchhoff plate theory is considered. On the basis of the Kirchhoff plate theory, the displacements at any material point in the plate are given by

$$u = -z\frac{\partial w(r,t)}{\partial r},\quad v=0,\quad w=w(r,t) \tag{9}$$

Where $w(r,t)$ is the displacement of the middle surface of the nanoplate at the point $(r,\theta,0)$.The size-dependent theories are utilized to predict accurately the mechanical behavior of the engineering structures in the nanoscale. The classical continuum theory is independent on the structure size. Thus, the classical continuum theory has a weakness to analyses of the nanostructures. To overcome this weakness, the classical continuum theory is modified and the modern continuum theories are existed. In this work, the modified couple stress theory is employed to analyze the nonlinear vibration behavior of FG circular and annular nanoplate. In comparison with the MCST, the MSGT contains two additional gradient tensors of the dilatation and the deviator stretch in addition to the symmetric rotation gradient tensor. Three independent material length scale parameters and two classical material constants for isotropic linear elastic materials are used to specify these tensors. For a continuum constructed by a linear elastic material occupying region Ω with infinitesimal deformations, the stored strain energy U_m can be defined as:

$$U_m = \frac{1}{2}\int_{\Omega}\left(\sigma_{ij}\varepsilon_{ij} + p_i\gamma_i + \tau^{(1)}_{ijk}\eta^{(1)}_{ijk} + m^{(1)}_{ij}\chi^{(1)}_{ij}\right)dv \tag{10}$$

in which the components of the strain tensor ε_{ij} ,the dilatation gradient tensor γ_i , the deviator stretch gradient tensor $\eta^{(1)}_{ijk}$, and the symmetric rotation gradient tensor $\chi^{(1)}_{ij}$ are given as [43].

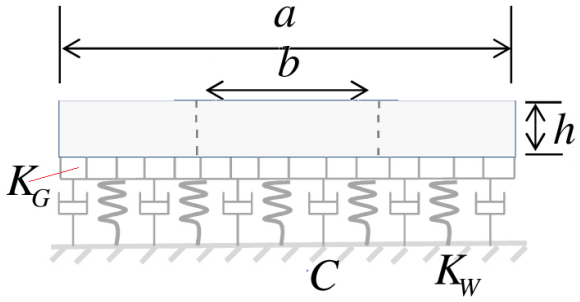

Fig.3. Functionally graded circular and annular nanoplate embedded on a Visco-Pasternak foundation.

The parameters λ and μ denote the Lame constants, respectively which are given as Eq.11 [44].

$$\lambda(z) = \frac{\upsilon(z)E(z)}{(1-\upsilon(z)^2)},\quad \mu(z) = \frac{E(z)}{2(1+\upsilon(z))} \tag{11}$$

By substituting the components of strain tensor, dilatation gradient tensor, deviator stretch gradient tensor, and symmetric rotation gradient tensor, the corresponding components of classical and nonclassical stresses can be evaluated. Therefore, the strain energy Π_S and kinetic energy are as Eq.12.

$$\Pi_s = \frac{1}{2}\int_A \begin{pmatrix} -M_r w_{,rr} - M_\theta\frac{1}{r}\frac{\partial w}{\partial r} + Y_{r\theta}(\frac{1}{r}\frac{\partial w}{\partial r} - \frac{\partial^2 w}{\partial r^2}) \\ -M^p_r(\frac{\partial^3 w}{\partial r^3} - \frac{1}{r^2}\frac{\partial w}{\partial r} + \frac{1}{r}\frac{\partial^2 w}{\partial r^2}) \\ -P_z(\frac{\partial^2 w}{\partial r^2} + \frac{1}{r}\frac{\partial w}{\partial r}) - T^\tau_{rrz}\frac{\partial^2 w}{\partial r^2} - \\ M^\tau_{rrr}\frac{\partial^3 w}{\partial r^3} + M^\tau_{\theta\theta r}(\frac{1}{r^2}\frac{\partial w}{\partial r} - \frac{1}{r}\frac{\partial^2 w}{\partial r^2}) - \frac{T^\tau_{\theta\theta z}}{r}\frac{\partial w}{\partial r} \end{pmatrix} dA$$

$$\Pi_T = \frac{1}{2}\int_A\left(I_1\left(\frac{\partial w}{\partial t}\right)^2 + I_2\left(\frac{\partial^2 w}{\partial r\partial t}\right)^2\right)dA \tag{12}$$

Where A denotes the area occupied by the mid-plane of the circular FG nanoplate. Furthermore, I_1 and I_2 are represented as the following form.

$$I_2 = \int_{-h/2}^{h/2}\rho(z)dz,\quad I_1 = \int_{-h/2}^{h/2}\rho(z)z^2dz \tag{13}$$

In Eq. (12), couple moments, bending moments, other higher-order resultants force and higher-order moments caused by higher-order stresses effective on the section are introduced as [55] and supplementary materials.

The work done by external forces can be expressed as Eq.14

$$W_{ext} = \int q\,w(r,t) + f\,w(r,t)$$

$$q = q_z + q_0 \tag{14}$$

Here q_0 and q_z are the distributed external force and Lorentz force respectively, f is the reaction force of elastic medium. The reaction force of the foundation is modeled as three different models. These models are linear Winkler, linear Winkler–Pasternak, and visco Winkler–Pasternak foundation. The formulation of these foundations is stated as:

$$f = K_w w(r,t) \qquad \text{The winkler foundation} \tag{15}$$

$$f = K_w w(r,t) - K_G\nabla^2 w(r,t) \qquad \text{The Pasternak foundation}$$

$$f = K_w w(r,t) - K_G\nabla^2 w(r,t) + C_d\frac{\partial w(r,t)}{\partial t} \qquad \text{Visco-Pasternak}$$

Using Hamilton's principle $\int_{t_1}^{t_2}(\Pi_s - \Pi_T - W_{ext})dt = 0$ and taking the variation of w , integrating by parts and setting the coefficients of δw equal to zero leads to the following governing equation and the boundary conditions. Eq.16 and Eq.17.

$$\delta w = 0 \quad \text{or} \quad -M_r - rM_{r,r} + M_\theta - 2Y_{r\theta}$$

$$-rY_{r\theta,r} + M^p_{r,r} + rM^p_{r,rr} - \frac{M^p_r}{r} - rP_{z,r} - T^\tau_{rrz}$$

$$-rT^\tau_{rrz,r} + T^\tau_{\theta\theta z} + 2M^\tau_{rrr,r} + rM^\tau_{rrr,rr} - M^\tau_{\theta\theta r} - M^\tau_{\theta\theta r,r} = 0$$

$$\frac{\partial\delta w}{\partial r} = 0 \quad \text{or} \quad rM_r + rY_{r\theta} - rM^p_{r,r} + rP_z + rT^\tau_{rrz}$$

$$-M^\tau_{rrr} - rM^\tau_{rrr,r} + M^\tau_{\theta\theta r} = 0$$

$$\frac{\partial^2\delta w}{\partial r^2} = 0 \quad \text{or} \quad rM^p_r + rM^\tau_{rrr} = 0 \tag{16}$$

$$\left\{2l_0^2+\frac{4l_1^2}{5}\right\}A'\frac{\partial^6 w}{\partial r^6}+\left\{\frac{6l_0^2}{r}+\frac{12l_1^2}{5r}\right\}A'\frac{\partial^5 w}{\partial r^5}$$
$$-\left\{C'+l_2^2B'+2l_0^2B'+\frac{2l_1^2}{15r^2}A'+\frac{8l_1^2}{15}B'\right\}\frac{\partial^4 w}{\partial r^4}$$
$$-\left\{\begin{matrix}\frac{2}{r}C'+\frac{2l_2^2}{r}B'+\frac{4l_0^2}{r}B'+\frac{12l_0^2}{r^3}A'-\\ \frac{16l_1^2}{15r}B'+\frac{4l_1^2}{15r^3}A'\end{matrix}\right\}\frac{\partial^3 w}{\partial r^3}$$
$$+\left\{\begin{matrix}\frac{1}{r^2}C'+\frac{l_2^2}{r^2}B'-\frac{18l_0^2}{r^4}A'+\frac{2l_0^2}{r^2}B'+\\ \frac{8l_1^2}{15r^2}B'+N_0+N^*+K_G\end{matrix}\right\}\frac{\partial^2 w}{\partial r^2}$$
$$+\left\{\begin{matrix}-\frac{1}{r^3}C'-\frac{l_2^2}{r^3}B'+\frac{18l_0^2}{r^5}A'-\frac{2l_0^2}{r^3}B'\\ -\frac{8l_1^2}{15r^3}B'+\frac{12l_1^2}{15r^4}A'+\frac{N_0}{r}+\frac{N^*}{r}+\frac{K_G}{r}\end{matrix}\right\}\frac{\partial w}{\partial r}$$
$$-K_w w-C_d\frac{\partial w}{\partial t}+\mu H_r{}^2\frac{\partial}{\partial t}\left(\frac{w}{r}+\frac{\partial w}{\partial r}\right)$$
$$=I_1\frac{\partial^2 w}{\partial t^2}-I_2\frac{\partial^4 w}{\partial t^2\partial r^2} \qquad (17)$$

Where, A', B' and C' are represented as [55].

A FG circular and annular nanoplate is considered to be resting on a Visco-Pasternak elastic foundation. The geometric properties of the nanoplate are demonstrated by outer radius *a*, inner radius *b*, thickness *h*. The following non-dimensional parameters are introduced for convenience and generality.

$$W=\frac{w}{a},\ \xi=\frac{r}{a},\ \zeta=\frac{r}{b},\ \beta=\frac{b}{a},\ \psi_i=\frac{l_i}{h},$$
$$\beta_0=\frac{B'l_0^2}{C'},\ \beta_1=\frac{B'l_1^2}{C'},\ \beta_2=\frac{B'l_2^2}{C'},\ \overline{\mathrm{K}}_W=\frac{K_W a^4}{C'}$$
$$\overline{\mathrm{C}}=\frac{C_d a^2}{C'}\sqrt{\frac{C'}{D'}},\ \overline{\mathrm{K}}_G=\frac{K_G a^2}{C'},\ \overline{\mathrm{P}}=\frac{N_0 a^2}{C'}$$
$$\mathrm{P}^*=\frac{N_0 a^2}{C'},\ \lambda=\frac{A'}{C'},\ \Omega^2=D'\frac{\omega^2 a^4}{C'},\chi^2=\frac{E'}{D'}$$
$$\tau=\frac{t}{a^2}\sqrt{\frac{C'}{D'}} \qquad (18)$$

Employing the above expressions, a non-dimensional differential equation for vibration of FG circular and annular nanoplate in thermal environment and magnet field can be obtained as Eq.19.

One can insert the size dependent parameters set equal to zero ($l_0=l_1=l_2=0$), In order to obtain the governing equation of the classical FG circular and annular plate. Moreover, with the assumption $l_0=l_1=0$ in the Eq. (24) the governing equation of the circular and annular plate will be obtained by the MCST. The Eq. 24 is rewritten as the following form Eq.25.

$$\left\{2\psi_0^2\lambda+\frac{4\psi_1^2}{5}\lambda\right\}\frac{\partial^6 W}{\partial\xi^6}+\left\{\frac{6\psi_0^2}{\xi}\lambda+\frac{12\psi_1^2}{5\xi}\lambda\right\}\frac{\partial^5 w}{\partial\xi^5}$$
$$-\left\{1+\beta_2+2\beta_0+\frac{2\psi_1^2}{15\xi^2}\lambda+\frac{8}{15}\beta_1\right\}\frac{\partial^4 w}{\partial\xi^4}$$
$$-\left\{\begin{matrix}\frac{2}{\xi}+\frac{2}{\xi}\beta_2+\frac{4}{\xi}\beta_0+\frac{12\psi_0^2}{\xi^3}\lambda-\frac{16}{15\xi}\beta_1\\ +\frac{4\psi_1^2}{15\xi^3}\lambda\end{matrix}\right\}\frac{\partial^3 w}{\partial\xi^3}$$
$$+\left\{\begin{matrix}\frac{1}{\xi^2}+\frac{1}{\xi^2}\beta_2-\frac{18\psi_0^2}{\xi^4}\lambda+\frac{2}{\xi^2}\beta_0+\\ \frac{8}{15\xi^2}\beta_1+\overline{\mathrm{P}}+\mathrm{P}^*+\overline{\mathrm{K}}_G\end{matrix}\right\}\frac{\partial^2 w}{\partial\xi^2}$$
$$+\left\{\begin{matrix}-\frac{1}{\xi^3}-\frac{1}{\xi^3}\beta_2+\frac{18\psi_0^2}{\psi^5}\lambda-\frac{2}{\xi^3}\beta_0\\ -\frac{8}{15\xi^3}\beta_1+\frac{12\psi_1^2}{15\xi^4}\lambda+\frac{\overline{\mathrm{P}}}{\xi}+\frac{\mathrm{P}^*}{\xi}+\frac{\overline{\mathrm{K}}_G}{\xi}\end{matrix}\right\}\frac{\partial w}{\partial\xi}$$
$$-\overline{\mathrm{K}}_W W-\overline{C}\frac{\partial W}{\partial\tau}-\frac{I_1 a^4}{C'}\frac{\partial^2 W}{\partial\tau^2}+$$
$$\frac{I_2 a^2}{C'}\frac{\partial^4 W}{\partial\tau^2\partial\xi^2}+\overline{f}_z=0 \qquad (19)$$

$$[M]\{\ddot{d}\}+[C]\{\dot{d}\}+[K]\{d\}=0 \qquad (20)$$

In the above equation, the matrices $[M]$, $[C]$ and $[K]$ are the mass, damper and stiffness matrix, respectively. By defining the new freedom vector and general solution of the Eq. 19 as the following form Eq.21

$$\{Q\}=\begin{Bmatrix}d\\ \dot{d}\end{Bmatrix},\qquad \mathrm{W}(\mathrm{r},\tau)=\{Q\}e^{\eta\tau} \qquad (21)$$

Using the Eq. (21), we can rewrite the Eq. (20) as

$$\left(\eta[A]+[B]\right)\{Q\}=0,\quad [A]=\begin{bmatrix}[0] & [M]\\ [I] & [0]\end{bmatrix}$$
$$[B]=\begin{bmatrix}[K] & [C]\\ [0] & -[I]\end{bmatrix} \qquad (22)$$

In the Eq.22, the η is a complex number and the vibration frequency of the FG circular and annular nanoplate is the imaginary part of the η. The elements of the stiffness, mass and damper matrix are given in [55].

4. Solution procedure

4.1. Solution FG circular nanoplate by Galerkin method

The Galerkin method has been widely used for the analysis of mechanical behavior of the structural elements at large and small scales, such as static, dynamic and stability problems [45,46] Since this numerical method provides simple formulation and low computational cost. Moreover, it is more general than the Rayleigh–Ritz method because no quadratic functional or virtual work principle is necessary. The Galerkin's method is used to change the nonlinear partial differential equation to a nonlinear ordinary differential equation. To this end, one can easily obtain

$$\iint_{\Omega} \bar{Q}\left(\sum_{j=1}^{n} A_j f_j(\xi)\right) f_k(\xi)\, d\Omega \qquad (23)$$

Where $f_j(\xi)\ (j=1,2,...,n)$ are the basic functions which must satisfy all boundary conditions, but not necessarily satisfy the governing equation. $A_j\ (j=1,2,...,n)$ are unknown coefficients to be determined. The integration extends over the entire domain of the plate Ω. The symbol $\bar{Q}$ indicates a differential operator and is the right-hand side of Eq. (23). Here, the boundary conditions (BC) are assumed to be clamped for the FG circular of constant thickness along the edge $\xi = 1$. The boundary conditions are written as w and it's the first derivative are zero at $\xi = 1$. In the Galerkin method, the lateral deflection can be determined by a linear combination of the basic functions for the numerical solutions of the problem under investigation. The basic functions must satisfy all the above-mentioned boundary conditions. The chosen basic function for $W(\xi)$ are.

$$f_j(\xi) = \xi^{2(j-1)}\left(1-\xi^2\right)^2 \qquad (24)$$

Using Eq. (23), Eq. (24) and (22), one can achieve the following system of linear algebraic equations.

$$\left(\left[B^*\right]+\eta\left[A^*\right]\right)\{Q\}=0$$

$$A^*_{k,j} = \int_0^1 \xi^{2k-1}\left(1-\xi^2\right)^2 G_{p1}\, d\xi$$

$$G_{p1} = \begin{bmatrix} [0] & c_1 \\ c_2 & [0] \end{bmatrix}$$

$$c_1 = [M]\left(\xi^{2(j-1)}\left(1-\xi^2\right)^2\right)$$

$$c_2 = [I]\left(\xi^{2(j-1)}\left(1-\xi^2\right)^2\right)$$

$$B^*_{k,j} = \int_0^1 \xi^{2k-1}\left(1-\xi^2\right)^2 G_{p2}\, d\xi$$

$$G_{p2} = \begin{bmatrix} [h_1] & [h_2] \\ [0] & [h_3] \end{bmatrix}$$

$$h_1 = [K]\left(\xi^{2(j-1)}\left(1-\xi^2\right)^2\right)$$

$$h_2 = [C]\left(\xi^{2(j-1)}\left(1-\xi^2\right)^2\right)$$

$$h_3 = -[I]\left(\xi^{2(j-1)}\left(1-\xi^2\right)^2\right) \qquad (25)$$

Here M, C and I are differential operators, which are given in [50].

4.2. DQM Solution

In this study, the differential quadrature method (DQM) [55] method is used to calculate the spatial derivatives of field variables in the equilibrium equations. The differential quadrature method (DQM) is a more efficient method, with acceptable accuracy and using less grid points. DQ technique can be applied to deal with complicated problems reasonably well because its implementation is very simple. In this approach, the problem formulation becomes simpler and also low computational efforts are required to obtain acceptable solutions in comparison with other approximate numerical methods such as the finite elements method (FEM), the finite difference method, the boundary element method and the mesh less methods. Moreover, DQ method is free of the shear locking phenomenon that occurs in the FEM because of discretizing the strong form of the governing equations and the related boundary conditions. Also, some other advantages and disadvantages of the DQ technique are reported in the review paper of Bert and Malik [56]. DQ approach has been utilized by many researchers for analyzing nanostructure elements, such as elastic buckling of single-layered graphene sheets. According to DQ method, the partial derivatives of a function $f(r)$ as an example, at the point (r_i) are expressed as [56].

Where the number of grid points in the r direction and the

$$\frac{d^s f(r)}{dr^s}\Big|_{r=r_i} = \sum_{j=1}^{n} C_{ij}^s f(r_j),\quad i=1,2,...,n \qquad (26)$$

respective weighting coefficient related to the s th-order derivative are n and C_{ij}^s respectively. According to Shu and Richard rule [46].

How to select the grid points is a key point in the successful application of differential quadrature method. It has been shown that the grid point distributions which is based on well accepted Gauss-Chebyshev–Lobatto points, gives sufficiently accurate results. According to this grid point's distribution, the grid point distribution in the ζ direction for annular and circular FG nanoplate are given in [56].

$$\zeta_i = \frac{1}{2}\left[1-\cos\left(\frac{i-1}{n-1}\pi\right)\right],\quad i=1,2,...,n \qquad (27)$$

The non-dimensional computational domain of the nanoplate is $0 \le \zeta \le 1$.

By direct substitution boundary conditions into the discrete governing equation, they are incorporated in the analysis [55]. Moreover, the derivatives in the boundary conditions are discretized by the DQ procedure. After implementation of the boundary conditions, M, C and I can be written in the following form Eq.28.

$$[C]=-\bar{C}W_i \tag{28}$$

$$[M]=+\frac{I_2a^2}{C'}\sum_{j=2}^{n-1}\hat{C}_{ij}^{2}W_j-\frac{I_1a^4}{C'}W_i$$

$$[K]=\left\{2\psi_0^2\lambda+\frac{4\psi_1^2}{5}\lambda\right\}\sum_{j=2}^{n-1}\hat{C}_{ij}^{6}W_j$$

$$+\left\{\frac{6\psi_0^2}{\xi}\lambda+\frac{12\psi_1^2}{5\xi}\lambda\right\}\sum_{j=2}^{n-1}\hat{C}_{ij}^{5}W_j$$

$$-\left\{\begin{matrix}1+\beta_2+2\beta_0\\+\frac{2\psi_1^2}{15\xi^2}\lambda+\frac{8}{15}\beta_1\end{matrix}\right\}\sum_{j=2}^{n-1}\hat{C}_{ij}^{4}W_j-\overline{\mathrm{K}}_W W_i$$

$$-\left\{\begin{matrix}\frac{2}{\xi}+\frac{2}{\xi}\beta_2+\frac{4}{\xi}\beta_0+\frac{12\psi_0^2}{\xi^3}\lambda\\-\frac{16}{15\xi}\beta_1+\frac{4\psi_1^2}{15\xi^3}\lambda\end{matrix}\right\}\sum_{j=2}^{n-1}\hat{C}_{ij}^{3}W_j$$

$$+\left\{\begin{matrix}\frac{1}{\xi^2}+\frac{1}{\xi^2}\beta_2-\frac{18\psi_0^2}{\xi^4}\lambda+\frac{2}{\xi^2}\beta_0\\+\frac{8}{15\xi^2}\beta_1+\overline{\mathrm{P}}+\mathrm{P}^*+\overline{\mathrm{K}}_G\end{matrix}\right\}\sum_{j=2}^{n-1}\hat{C}_{ij}^{2}W_j$$

$$+\left\{\begin{matrix}-\frac{1}{\xi^3}-\frac{1}{\xi^3}\beta_2+\frac{18\psi_0^2}{\psi^5}\lambda-\frac{2}{\xi^3}\beta_0\\-\frac{8}{15\xi^3}\beta_1+\frac{12\psi_1^2}{15\xi^4}\lambda+\frac{\overline{\mathrm{P}}}{\xi}+\frac{\mathrm{P}^*}{\xi}+\frac{\overline{\mathrm{K}}_G}{\xi}\end{matrix}\right\}\sum_{j=2}^{n-1}\hat{C}_{ij}^{1}W_j$$

.

Where,

$$\bar{\Sigma}_i^s=\sum_{j=2}^{n-1}\hat{C}_{ij}^{s}W_j,\quad \hat{C}_{ij}^{s}=C_{ij}^{s}-C_{i1}^{s}C_{nj}^{1}/C_{n1}^{1}$$

$$\text{for } i=1,2,...,n \text{ and } s=1,2,...,6 \tag{29}$$

After employing the aforementioned solution procedure, one achieves the following system of linear algebraic equations:

$$\left(\eta[A]+[B]\right)\{Q\}=0 \tag{30}$$

Where $[A]$ and $[B]$ are $(n-2)\times(n-2)$ square matrices, which are easily extracted. Furthermore, the non-dimensional buckling load η can be calculated from the eigenvalues of an algebraic equations system. This parameter is a complex number that the imaginary part is the vibration frequency of the FG circular and annular nanoplate.

5. Result and discussions

Magnet-thermo vibration analysis of FG circular and annular nanoplate based on modified couple stress theory and modified strain gradient theory is discussed here according to the formulas obtained above. The effects of the main parameters including the small scale parameters, magnetic field, temperature change and their combinations on the natural frequencies are investigated. Properties of FG circular and annular nanoplate in this paper are considered as follows:

$E_m=70$ GPa, $\alpha_m=23\times10^{-6}$, $\rho_m=2702\ kg/m^3$

$\upsilon_m=0.3$, $\mu=1.256665081E-6$ $[\frac{H}{m}]$

$E_c=427$ GPa, $\alpha_c=7.4\times10^{-6}$, $\rho_c=3100\ kg/m^3$

The existing local plate model solutions are applied to verify the accuracy of circular and annular results. Following four boundary conditions have been considered in the vibration analysis of the annular graphene sheets.

SC: Annular graphene sheet with simply supported outer and clamped inner radius.

SS: Annular graphene sheet with simply supported outer and inner radius.

CC: Annular graphene sheet with clamped outer and inner radius.

CS: Annular graphene sheet with clamped outer and simply supported inner radius.

5.1 Validation of the work

In this section, the present work is compared with the reported results in the literature. To this end, in order to compare the numerical results, it is assumed that the nonlocal parameter is set to zero and the model can easily reduce to the classical circular and annular plate model. To confirm the reliability of the present formulation and results, comparison studies are conducted for the natural frequencies of the circular plate by ignoring size dependent parameters. The comparison of the vibration frequency parameters for circular plates is tabulated in table 1. It is observed that the present results are in excellent agreement with the classical results.

The comparison of natural frequency is presented in table 2 for the annular plates. The obtained results for nanoplate in table 2 are in good agreement with those non-dimensional natural frequency values by previous researchers [53, 56].

Although DQ method is a highly efficient method by using a small number of grid point, but it is not efficient when the number of grid points is large and it is also sensitive to grid point distribution. To establish the numerical algorithm as well as convergence of the present results, the non-dimensional natural frequencies of FG circular and annular nanoplate embedded in various elastic medium corresponding to different numbers of grid points are plotted in fig.4. The radius of nanoplate, size dependent parameter, the shear, Winkler and damping coefficients are 20 nm, 0.5 nm, 5, 80 and 5, respectively. According to the Fig.4, it is remarked that the number of grid points is considered as (N_ξ=11).

Since there are no published results available for annular nanoplates in open literature, the results of annular microplate are used for comparison. To obtain these results, the modified couple stress theory is utilized. From this table, one can see that the present results are in good agreement with the reported

Results in the literature. To obtain the natural frequencies of the FG annular plate, the boundary condition of annular microplate are assumed SS and CC. The other material properties of the annular microplate are reported by Ke et al. [57].

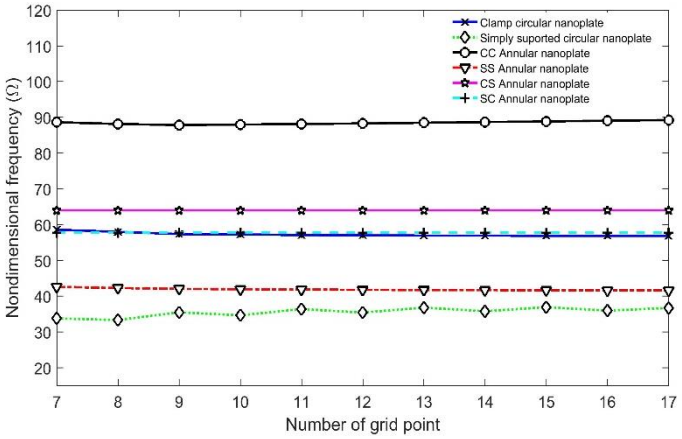

Fig. 4 Convergence study and minimum number of grid points (N_ζ) required to obtain accurate results.

5.2 Numerical Results

Numerical analyses for the magneto-thermo-mechanical free vibrational characteristics of FG circular and annular nanoplates with various elastic foundations and boundary conditions are performed using the proposed MCST and NSGT plate model and presented solution methodology. It is intended to study the influences of important parameters such as the non-dimensional nonlocal parameter, temperature change, external magnetic potential and type of edge support on the natural frequency of FG circular and annular nanoplates **Fig**.5 shows the variation of vibration frequency versus compressive in-plane pre-load for FG annular nanoplate. The non-dimensional parameters of elastic foundation such as shear modulus parameter $\overline{K}_G$, Winkler modulus parameter $\overline{K}_W$ and damping modulus of damper $\bar{c}$ for the surrounding polymer matrix are considered to 5, 80 and 5 respectively as well as the magnetic field parameters are considered based on [58]. The results show that the vibration frequency is sensitive to the modulus of the surrounding elastic medium and decreases by increasing the in-plane pre-load as well as increases by increasing the magnetic field effect. Furthermore, it is shown that the damping modulus gives rise to decrease the vibration frequency. Therefore, the FG nanoplate based on the Pasternak and Visco-Winkler medium have the greatest and the smallest vibration frequency, respectively. Figure 6 shows the natural frequencies of the FG circular nanoplate under magnetic field for four different boundary conditions, when different values of aspect ratio are considered to determine the effect of the aspect ratio on the vibration frequency of the FG nanoplate. To obtain the results, the power index parameter, inner radius, the size dependent parameter of MSGT and magnetic field parameters are considered to 7, 30 nm, 0.5h and the data based on [58] respectively. Fig. 6 illustrates the non-dimensional frequency increases with the increase of aspect ratio and also the non-dimensional frequency increases monotonically by increasing the rigidity of boundary conditions. Moreover, the Fig. 6 shows that increasing the aspect ratio gives rise to increase the gap between the curves.

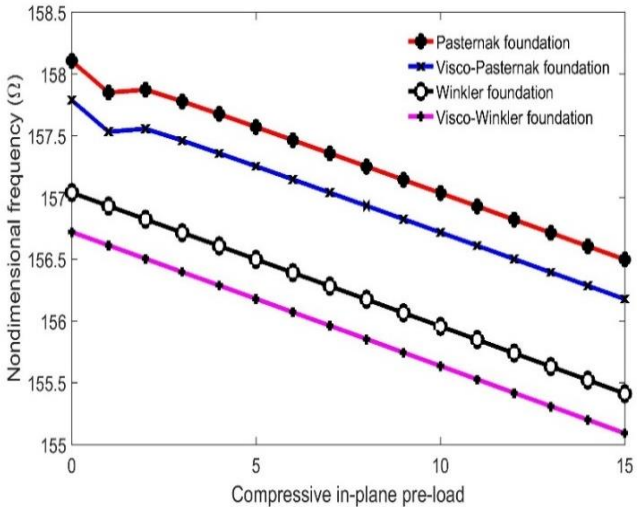

Fig. 5 Variation of vibration frequency of annular with the compressive pre-load for various kind of elastic medium.

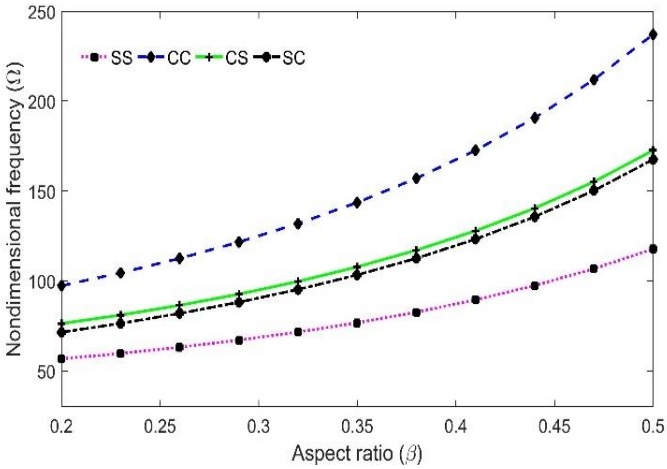

Fig. 6 Variation of vibration frequency with the aspect ratio for annular by various boundary conditions

The Fig.7a and Fig.7b illustrate the first vibration frequencies of the annular and circular FG nanoplate respectively. In this figure, for different temperature changes and magnetic field parameters, the dependency of vibration frequency versus the radius of annular FG nanoplate is observed. To obtain the results, it is supposed that the FG nanoplate resting on a visco-Pasternak medium and the shear elastic, Winkler elastic and external damping coefficient are considered to 5, 80 and 5, respectively. Moreover, the power index of FG material and the size dependent length of FG circular nanoplate are specified to 5, and 0.5h, respectively. By employing the modified strain gradient theory, the vibration frequencies of FG annular nanoplate are extracted. From the Fig.7 it is obvious that the vibration frequency of FG circular nanoplate is strongly depend on the nanoplate radius and this dependency is more for the larger temperature change. Moreover, diminishing nanoplate radius causes to decrease the effects of temperature change. Also, the temperature changes have a decreasing effect on the vibration frequency of circular nanoplate. In contrast, the Magnetic field has an increasing effect on the vibration frequency of circular and annular nanoplate.

Table 1 Comparison of the present results with natural frequency parameters of classical plate theory $\Omega=\sqrt{\rho h/C'}\omega a^2$

	References					
Boundary condition	Leissa and Narita [59]	Kim and Dickinson [60]	Qiang [61]	Zhou et al. [62]	Present	
simply supported boundary condition	13.898	13.898	13.898	13.898	13.898	
clamped boundary condition	Leissa [59]	Kim and Dickinson [60]	Qiang [61]	Zhou et al. [62]	Present (DQM)	Present (Galerkin)
	21.26	21.26	21.26	21.26	21.26	21.26

Table 2 Comparison of the present results with classical plate theory for the lowest six natural frequency parameters $\left(\Omega=\omega a^2\sqrt{\rho h/C'},\ \beta=b/a=0.4\right)$

	References		
Boundary condition	Li and Li [61]	Zhou et al [62]	Present
CC	63.04	62.996	62.979
SS	30.09	30.079	30.084
SC	42.63	42.548	42.569
CS	46.74	46.735	46.743

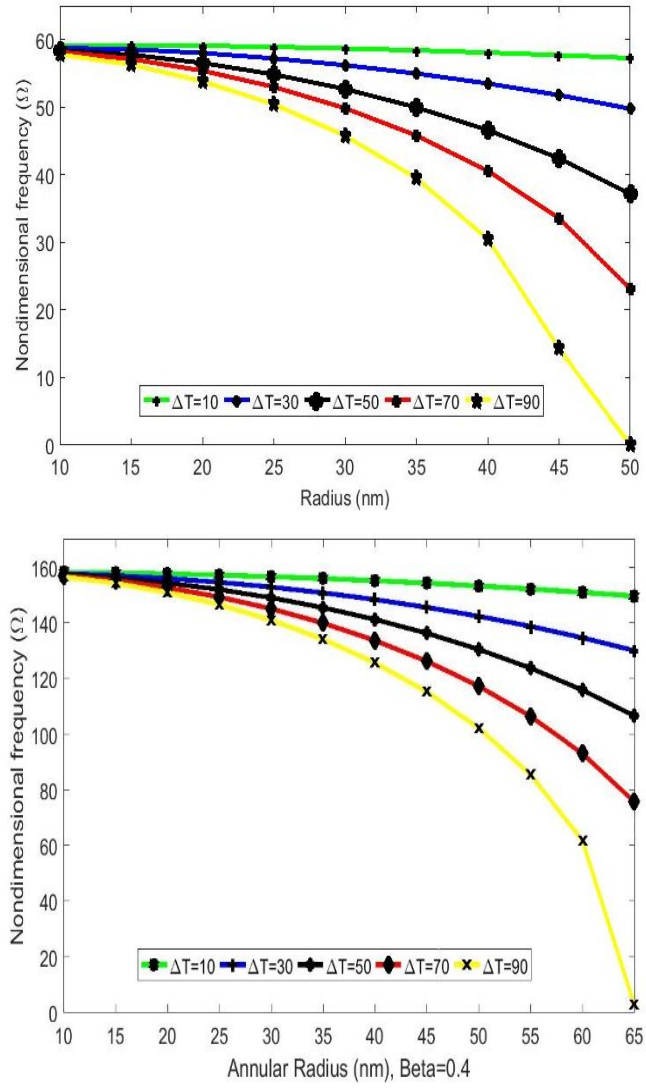

Fig. 7. Variation of vibration frequency with the radius of annular (a) and circular (b) FG nanoplate (Clamp-Clamp) under magnet field and various temperature changes.

According to the figure.7, the natural frequency is strongly depend to the radius of FG nanoplate and this parameter has a decreasing effect on the nanoplate natural frequency. Furthermore, as the vibration frequency becomes zero in a specific radius and temperature change in, there are a critically temperature and radius for FG nanoplate. Therefore, these specific radius and temperature change are called the critically parameters. It is necessary to note that the effect of magnetic field has an increasing effect on nondimensional natural frequency.

Depicted in fig.8a and fig8.b are the influence of nondimensional nonlocal parameter under magnetic field based on [58] and the temperature change of ΔT=50 by considering the modified couple stress and the modified strain gradient theory on the vibration response of FG circular and annular nanoplate with various power index parameter. It can be found that as the size dependent parameter increases, the non-dimensional frequency increases for all values of the power index parameter. The fig.8 show that for all values of power index parameters the difference between MCST and MSGT results increase as the values of size dependent parameter increase. Moreover, the vibration frequency decreases as the power index parameter increases. Furthermore, as can be seen from Fig. 8, the non-dimensional frequency is sensitive to the size dependent parameter for small values of power index parameter and increases by increasing the value of magnetic field.

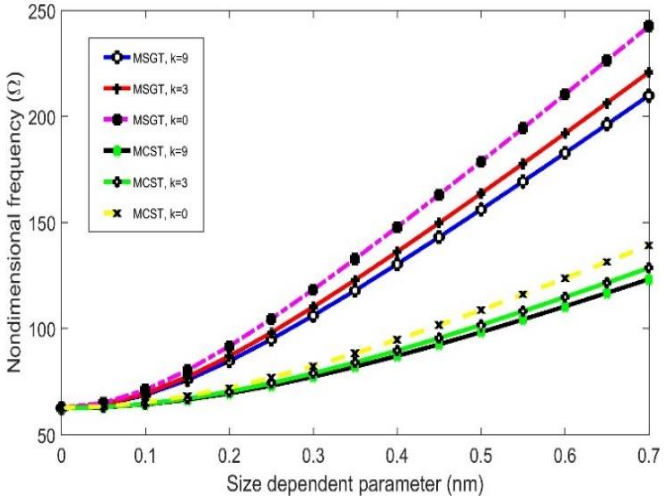

Fig. 8a. Variation of vibration frequency with the size dependent parameters of the FG circular (a) nanoplate for various power index parameter and two different elasticity

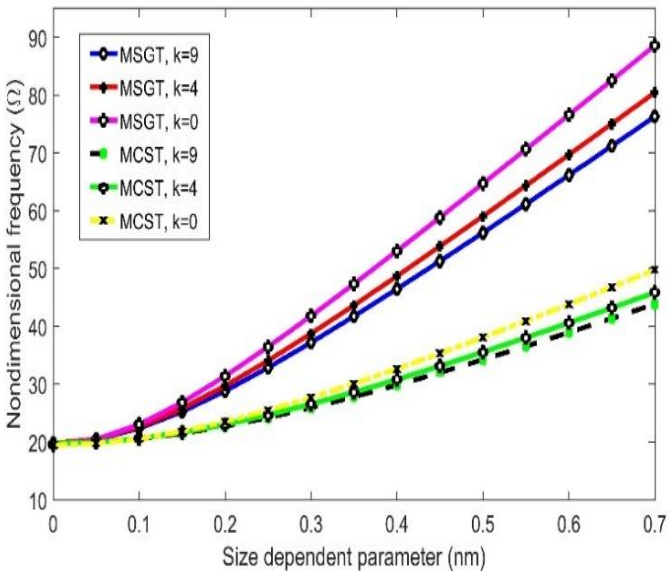

Fig. 8b. Variation of vibration frequency with the size dependent parameters of the FG annular (b) nanoplate for various power index parameter and two different elasticity

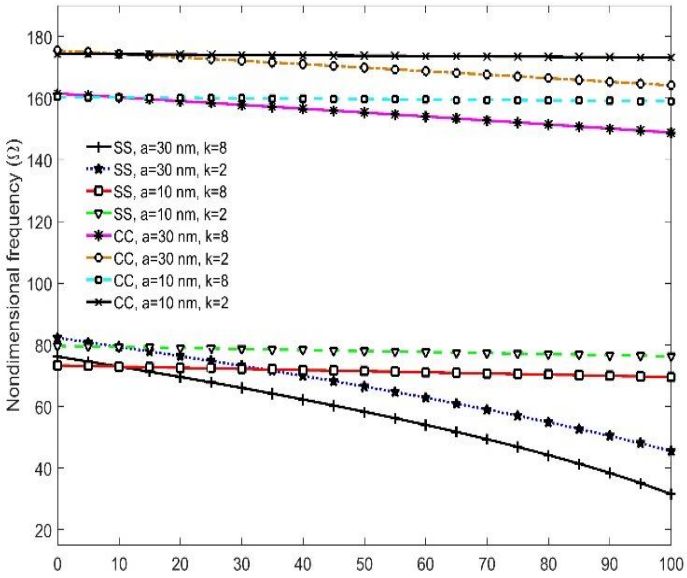

Fig.9b. Variation of vibration frequency of the FG annular (b) nanoplate for various power index parameter, radius and boundary conditions.

Fig.9a and Fig.9b highlight the influence of temperature changes on non-dimensional natural frequency with considering different power index, size effect parameters and magnetic field. The aspect ratio of nanoplate is considered 0.4. It is depicted that the non-dimensional frequency increases as the rigidity of the boundary condition for all lengths increases. Such vibration response is observed for other boundary conditions as well. Also, the results illustrate that low power index parameter leads to higher natural frequency of FG annular nanoplate in comparison with high power index parameter. Also, the value of nondimensional natural frequencies annular nanoplate under magnetic field is more than circular nanoplate. Moreover, it is shown that the effect of temperature change on the nondimensional frequency is significant for simply supported annular nanoplate with high power index parameter in comparison with the annular nanoplate with rigidity boundary condition and small power index parameter.

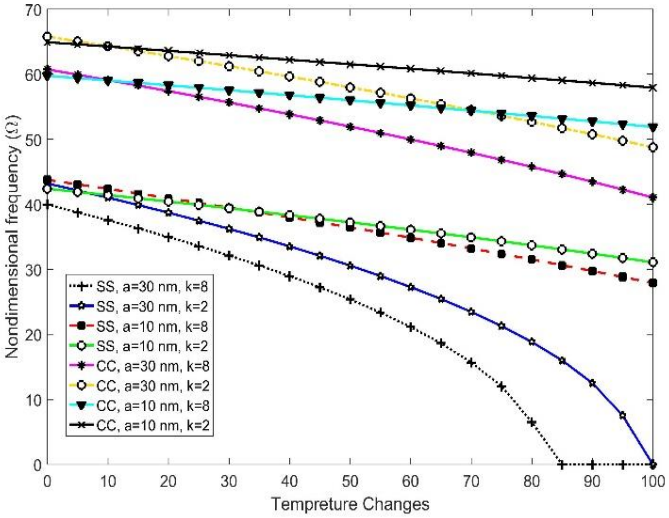

Fig.9a. Variation of vibration frequency of the FG circular nanoplate for various power index parameter, radius and boundary conditions.

6. Concluding remarks

The magneto-thermo-mechanical free vibration of FG circular and annular nanoplates with different boundary conditions was numerically studied. The FG circular and annular nanoplates were considered to be subjected to an applied magnetics potential and a uniform temperature change. The size-dependent mathematical formulation of FG circular and annular Nanoplate was extracted based on the modified couple stress theory and the modified strain gradient theory based on the Kirchhoff plate theory. The differential quadrature method and Galerkin method were utilized to calculate the natural frequencies of FG nanoplate. A parametric study was conducted to consider the influences of nondimensional nonlocal parameter, magnetic and thermal loadings and boundary conditions on the free vibration characteristics of FG circular and annular nanoplates. The importance of taking the small-scale effect into account was investigated by providing a direct comparison between the results predicted by the present nonlocal FG circular and annular nanoplate model with those by the classical continuum mechanics model. From the results, it was concluded that the nondimensional vibration frequency of FG circular and annular nanoplate is intensely depend on nanoplate radius and this dependency is more at high temperature change and magnetic field. Moreover, the non-dimensional natural frequency decreases at high temperature case. In contrast, the magnetic field has an increasing trend to non-dimensional natural frequency. Also, the effect of temperature change on nondimensional natural frequency is in contrast to low temperature case in comparison to high temperature. Furthermore, it is observed that the effect of power index parameter on the modified strain gradient theory is much more than the modified couple stress theory and also the power index parameter has a decreasing effect on the vibration frequency of FG circular and annular nanoplate. In addition, as the size dependent parameter increases, the differences between the vibration responses of the FG annular and circular nanoplate increase. Finally, changing the state of stress in both tangential and radial directions is caused by applying radial magnetic field to the top surface of the plate, which gives rise to change the natural frequency.

Acknowledgments

This research was supported by Shahid Chamran University, Faculty of mechanical engineering. We thank our colleagues from mechanical engineering of faculty who provided insight and expertise that greatly assisted the research.

References

1.Suresh, S., and Mortensen, A. 1998, Fundamentals of Functionally Graded Materials: Processing and Thermomechanical Behavior of Graded Metals and Metal-Ceramic Composites. London: IOM Communications Ltd.

2.Sallese, J.M., et al., 2001, Electrical modeling of a pressure sensor MOSFET, . Sens. Actuators A, Actuators A, Phys. . 94: p. 53-58.

3.Younis, M.I., Abdel-Rahman, E.M., and Nayfeh, A. 2003, A reduced-order model for electrically actuated microbeambased MEMS,. J. Microelectromech. Syst.. 12: p. 672–680.

4.Zhao, X.P., E.M. Abdel-Rahman, and A.H. Nayfeh, 2004, A reduced-order model for electrically actuated microplates,. J. Micromech. Microeng. 14: p. 900-906.

5.Coomar, N., Kadoli, R. 2010, Comparative analysis of steady state heat transfer in a TBC and functionally graded air cooled gas turbine blade", Sadhana Vol. 35, Part 1.

6. Nayfeh, A.H., M.I. Younis, and E.M. 2006, Abdel-Rahman, Dynamic pull-in phenomenon in MEMS resonators,. Nonlinear Dynamic. 48: p. 153–163.

7. Bharti, I., Gupta, N., and Gupta, K. 2013, Novel Applications of Functionally Graded Nano, Optoelectronic and Thermoelectric Materials International Journal of Materials, Mechanics and Manufacturing, Vol. 1, No. 3.

8. Jamian, S. 2012, Application of Functionally Graded Materials for Severe Plastic Deformation and Smart Materials : Experimental Study and Finite Element Analysis. Thesis submitted to Graduate School of Engineering, Nagoya Institute of Technology, Doctor degree of engineering.

9. Shishesaz, M., Zakipour, A., Jafarzadeh, A. 2016, Magneto-elastic analysis of an annular FGM plate based on classical plate theory using GDQ method. Latin Am. J. Solids Struct. 13(14), 2736–2762.

10. Wong E.W., Sheehan P.E., and Lieber C.M., 1997. Nanobeam mechanics: elasticity, strength and toughness of nanorods and nanotubes. Science, 277: p. 1971–1975.

11. Zhou S.J. and Li Z.Q., 2001, Metabolic response of Platynota stultana pupae during and after extended exposure to elevated CO2 and reduced O2 atmospheres. Shandong University Technology. 31: p. 401-409.

12.Akbaş, S.D. 2017, Free vibration of edge cracked functionally graded microscale beams based on the modified couple stress theory. Int J Struct Stab Dyn,17(03):1750033.

13.Danesh M., Farajpour A., and Mohammadi M., 2012, Axial vibration analysis of a tapered nanorod based on nonlocal elasticity theory and differential quadrature method. Mechanics Research Communications. 39: p. 23-27.

14.Mohammadi M., et al., 2012, Small scale effect on the vibration of orthotropic plates embedded in an elastic medium and under biaxial in-plane pre-load via nonlocal elasticity theory. Journal of Solid Mechanics. 4: p. 128-143.

15.Mohammadi M., et al., 2013. Influence of in-plane pre-load on the vibration frequency of circular graphene sheet via nonlocal continuum theory. Composites Part B. 51: p. 121–129.

16.Mohammadi M., et al., 2014, Exact solution for thermo-mechanical vibration of orthotropic mono-layer graphene sheet embedded in an elastic medium. Latin American Journal of Solids and Structures. 11(3): p. 437-458.

17.Nie, G. J. and Zhong, Z. 2007, Semi-analytical solution for three-dimensional vibration of functionally graded circular plates. Comput Method Appl.196(49-52):4901–4910.

18.Ke, L. L., Yang, J., and Kitipornchai, S. 2010, An analytical study on the nonlinear vibration of functionally graded beams. Meccanica;45(6):743–752.

19.Xia, X. K., and Shen, H. S. 2009, Comparison of vibration characteristics for postbuckled FGM plates with piezoelectric fiber reinforced composite actuators. Int J Struct Stab Dyn;9(03):533–559.

20.Akbaş, Ş. D. 2017, Free vibration of edge cracked functionally graded microscale beams based on the modified couple stress theory. Int J Struct Stab Dyn;17(03):1750033.

21.Lin, F., and Xiang, Y. 2014, Numerical analysis on nonlinear free vibration of carbon nanotube reinforced composite beams. Int J Struct Stab Dyn;14(01):1350056.

22.Hosseini-Hashemi, S., Taher, H. R. D. and Akhavan, H. 2010, Vibration analysis of radially FGM sectorial plates of variable thickness on elastic foundations. Compos Struct;92(7):1734–1743.

23.Shamekhi, A., and Nai, M. H. 2005, Buckling analysis of circular FGM plate having variable thickness under uniform compression by mesh free method. Int J Comp Meth;2(03):327–340.

24.Bayat, M., Sahari, B. B., and Saleem, M. 2012, The effect of ceramic in combination of two sigmoid unctionally graded rotating disks with variable thickness. Int J Comp Meth;9(02):1240029.

25. Tornabene, F., Fantuzzi, N., Bacciocchi, M., Viola, E., and Reddy, J. 2017, A numerical investigation on the natural frequencies of FGM sandwich shells with variable thickness by the local generalized differential quadrature method. Appl Sci;7(2):131.

26.Wang, B., J. Zhao, and Zhou, S., 2010, A micro scale Timoshenko beam model based on strain gradient elasticity theory. European Journal.Mech. A, Solids. 29: p. 591–599.

27.Ansari, R., R. Gholami, and S. Sahmani, 2011, Free vibration of size-dependent functionally graded microbeams based on a strain gradient theory. Composite Structures. 94: p. 221–228.

28.Ansari, R., R. Gholami, and S. Sahmani, 2012, Study of small scale effects on the nonlinear vibration response of functionally graded Timoshenko microbeams based on the strain gradient theory. ASME Journal Computational. Nonlinear Dynamics. 7: p. 031010

29.Sahmani, S. and R. Ansari, 2013, On the free vibration response of functionally graded higher-order shear deformable microplates based on the strain gradient elasticity theory. Composite Structures. 95: p. 430–442.

30.Ghayesh, M.H., M. Amabili, and H. Farokhi, 2013, Nonlinear forced vibrations of a microbeam based on the strain gradient elasticity theory. International Journal Engineering Science,. 63: p. 52–60.

31.Mohammadi M., et al., 2013, Shear buckling of orthotropic rectangular graphene sheet embedded in an elastic medium in thermal environment. Composites Part B.

32.Civalek Ö. and Akgöz B., 2013, Vibration analysis of micro-scaled sector shaped graphene surrounded by an elastic matrix. Computational Materials Science. 77: p. 295-303.

33.Murmu T. and Pradhan S. C., 2009, Vibration analysis of nano-single-layered graphene sheets embedded in elastic medium based on nonlocal elasticity theory. Journal Applied Physics: p. 105: 064319.

34.Pradhan S.C. and Phadikar J.K., 2009, Small scale effect on vibration of embedded multi layered graphene sheets based on nonlocal continuum models. Physics Letters A. 373: p. 1062–1069.

35.Wang Y. Z., Li F. M, and Kishimoto K., Thermal effects on vibration properties of double-layered nanoplates at small scales. Composite Part B Engineering. 42: p. 1311-1317.

36.Reddy C.D., Rajendran S., and Liew K.M., 2006, Equilibrium configuration and continuum elastic properties of finite sized graphene. Nanotechnology. 17: p. 864–870.

37.Aksencer T., Aydogdu M., and 2011, Levy type solution method for vibration and buckling of nanoplates using nonlocal elasticity theory. Physica. E43: p. 954 –959.

38.Malekzadeh P., Setoodeh A.R., and Alibeygi Beni A., 2011, small scale effect on the thermal buckling of orthotropic arbitrary straight-sided quadrilateral nanoplates embedded in an elastic medium. Composite Structure. 93: p. 2083–2089.

39.Satish N., Narendar S., and Gopalakrishnan S., 2012, Thermal vibration analysis of orthotropic nanoplates based on nonlocal continuum mechanics. Physica. E 44: p. 1950 –1962.

40.Prasanna Kumar T.J., Narendar S., and Gopalakrishnan S., 2013, Thermal vibration analysis of monolayer graphene embedded in elastic medium based on nonlocal continuum mechanics. Composite Structures. 100: p. 332–342.

41.Farajpour A., et al., 2011, Axisymmetric buckling of the circular graphene sheets with the nonlocal continuum plate model. Physica. E 43: p. 1820 –1825.

42.Mohammadi M., Ghayour M., and Farajpour A., 2013, Free transverse vibration analysis of circular and annular graphene sheets with various boundary conditions using the nonlocal continuum plate model. Composites Part B. 45: p. 32-42.

43.Bayat M., et al., 2014, One-dimensional analysis for magneto thermo mechanical response in a functionally graded annular variable thickness rotating disk. Applied Mathematical Modelling. 38: p. 4625-4639.

44.Behravan Rad A. and Shariyat M., 2015, Three-dimensional magneto-elastic analysis of asymmetric variable thickness porous

FGM circular plates with non-uniform tractions and Kerr elastic foundations. Composite Structures. 125: p. 4625-574.

45.Wang X. and Dai H.L., 2004, Magneto thermodynamic stress and perturbation of magnetic field vector in an orthotropic thermo-elastic cylinder. International Journal of Engineering Science. 42: p. 539-556.

46.Ghorbanpour A., et al., 2010, semi-analytical solution of magneto-thermo-elastic stresses for functionally graded variable thickness rotating disks. Journal of Mechanical Science and Technology. 24 (10): p. 2107-2117.

47.Daneshmehr, A., Rajapoor, A., and Hadi., A. 2015, Size dependent free vibration analysis of nanoplates made of functionally graded materials based on nonlocal elasticity theory with high order theories. International Journal of Engineering Science. 95: p. 23-35.

48.Zargaripoora, A., et al., 2018, Free vibration analysis of nanoplates made of functionally graded materials based on nonlocal elasticity theory using finite element method. Journal of Computational Applied Mechanics. 49.

49.Nejad, M.Z. and Hadi., A, 2016, Non-local analysis of free vibration of bi-directional functionally graded Euler-Bernoulli nano-beams. International Journal of Engineering Science. 105: p. 1-11.

50.Hosseini, M., et al., 2016, Stress analysis of rotating nano-disks of variable thickness made of functionally graded materials. International Journal of Engineering Science. 109: p. 29-53.

51.Nejad., M.Z. and Hadi., A.2016, Eringen's non-local elasticity theory for bending analysis of bi-directional functionally graded Euler-Bernoulli nano-beams. International Journal of Engineering Science. 106: p. 1-9.

52.Hosseini, M., et al., 2017, Size-dependent stress analysis of single-wall carbon nanotube based on strain gradient theory. International Journal of Applied Mechanics. 9: p. 1750087.

53.Zamani Nejad., M.J. Mohammad, and Hadi., A., 2017, A review of functionally graded thick cylindrical and conical shells. Journal of Computational Applied Mechanics. 48: p. 357-370.

54.Shishesaz, M., et al., 2017, Analysis of functionally graded nanodisks under thermoelastic loading based on the strain gradient theory. Acta Mechanica,. 228(12): p. 4141-4168.

55.Goodarzi, M., Mohammadi, M., Khooran, M., and Saadi, F. 2016 , "Thermo-Mechanical Vibration Analysis of FG Circular and Annular Nanoplate Based on the Visco-Pasternak Foundation" Journal of Solid Mechanics Vol. 8, No. 4 (2016) pp. 788-805..

56.Shu C., 2000, Differential quadrature and its application in engineering. Berlin: Springer, 2000.

57.Farajpour A., Danesh M., Mohammadi M., 2011, Buckling analysis of variable thickness nanoplates using nonlocal continuum mechanics, Physica Vol. 44, pp. 719–727.

58.Amiri, A., Fakhari, S.M., Pournaki, I.J., Rezazadeh, G., and Shabani, R. M. 2015, Vibration Analysis of Circular Magneto-electro-elastic Nano-plates based on Eringen's Nonlocal Theory. IJE TRANSACTIONS C: Aspects.Vol. 28, No. 12, (2015) 1808-181

59.Ke, LL., Wang, Y-S., Yang, J. 2014, Free vibration of size-dependent magneto-electro-elastic nanoplates based on the nonlocal theory. Acta Mechanica Sinica 30(4): 516–525.

60.Leissa A. W. and Narita Y., 1980, Natural frequencies of simply supported circular plates. Journal Sound Vibration. 70: p. 221–9.

61.Kim C. S and Dickinson S. M., 1989, on the free, transverse vibration of annular and circular, thin, sectorial plates subject to certain complicating effects. Journal Sound and Vibration. 134: p. 407–21.

62.Qiang., L.Y. and Jian., L, 2007, Free vibration analysis of circular and annular sectorial thin plates using curve strip Fourier P-element. Journal Sound and Vibration. 305: p. 457–66.

Supplementary Material

The components of the strain tensor ε_{ij}, the dilatation gradient tensor γ_i, the deviator stretch gradient tensor $\eta^{(1)}_{ijk}$, and the symmetric rotation gradient tensor $\chi^{(1)}_{ij}$ are given as [55].

$$\chi^{(s)}_{r\theta} = \frac{1}{2}\left(-\frac{\partial^2 w}{\partial r^2}+\frac{1}{r}\frac{\partial w}{\partial r}\right),$$
$$\gamma_r = -z\left(\frac{\partial^3 w}{\partial r^3}+\frac{1}{r}\frac{\partial^2 w}{\partial r^2}-\frac{1}{r^2}\frac{\partial w}{\partial r}\right),$$
$$\gamma_z = -\left(\frac{\partial^2 w}{\partial r^2}+\frac{1}{r}\frac{\partial w}{\partial r}\right)$$
$$\eta^{(1)}_{rrr} = \frac{z}{5}\left(\frac{1}{r}\frac{\partial^2 w}{\partial r^2}-\frac{1}{r^2}\frac{\partial w}{\partial r}-2\frac{\partial^3 w}{\partial r^3}\right),$$
$$\eta^{(1)}_{r\theta\theta} = \eta^{(1)}_{\theta\theta r} = \eta^{(1)}_{\theta r\theta} = \frac{z}{15}\left(3\frac{\partial^3 w}{\partial r^3}+\frac{4}{r^2}\frac{\partial w}{\partial r}-\frac{4}{r}\frac{\partial^2 w}{\partial r^2}\right)$$
$$\eta^{(1)}_{rrz} = \eta^{(1)}_{rzr} = \eta^{(1)}_{zrr} = \frac{1}{15}\left(\frac{1}{r}\frac{\partial w}{\partial r}-4\frac{\partial^2 w}{\partial r^2}\right),$$
$$\eta^{(1)}_{z\theta\theta} = \eta^{(1)}_{\theta\theta z} = \eta^{(1)}_{\theta z\theta} = \frac{1}{15}\left(\frac{\partial^2 w}{\partial r^2}-\frac{4}{r}\frac{\partial w}{\partial r}\right)$$
$$\eta^{(1)}_{rzz} = \eta^{(1)}_{zzr} = \eta^{(1)}_{zrz} = \frac{z}{15}\left(3\frac{\partial^3 w}{\partial r^3}-\frac{1}{r^2}\frac{\partial w}{\partial r}+\frac{1}{r}\frac{\partial^2 w}{\partial r^2}\right),$$
$$\eta^{(1)}_{zzz} = \frac{1}{5}\left(\frac{\partial^2 w}{\partial r^2}+\frac{1}{r}\frac{\partial w}{\partial r}\right) \qquad (31)$$

$$m^{(s)}_{r\theta} = \mu(z)l_2^2\left(-\frac{\partial^2 w}{\partial r^2}+\frac{1}{r}\frac{\partial w}{\partial r}\right),$$
$$p_r = -2z\mu(z)l_0^2\left(\frac{\partial^3 w}{\partial r^3}+\frac{1}{r}\frac{\partial^2 w}{\partial r^2}-\frac{1}{r^2}\frac{\partial w}{\partial r}\right),$$
$$p_z = -2\mu(z)l_0^2\left(\frac{\partial^2 w}{\partial r^2}+\frac{1}{r}\frac{\partial w}{\partial r}\right)$$
$$\tau^{(1)}_{rrr} = \frac{2z\mu(z)l_1^2}{5}\left(\frac{1}{r}\frac{\partial^2 w}{\partial r^2}-\frac{1}{r^2}\frac{\partial w}{\partial r}-2\frac{\partial^3 w}{\partial r^3}\right),$$
$$\tau^{(1)}_{rrz} = \tau^{(1)}_{rzr} = \tau^{(1)}_{zrr} = \frac{2\mu(z)l_1^2}{15}\left(\frac{1}{r}\frac{\partial w}{\partial r}-4\frac{\partial^2 w}{\partial r^2}\right)$$
$$\tau^{(1)}_{r\theta\theta} = \tau^{(1)}_{\theta\theta r} = \tau^{(1)}_{\theta r\theta} = \frac{2z\mu(z)l_1^2}{15}\left(3\frac{\partial^3 w}{\partial r^3}+\frac{4}{r^2}\frac{\partial w}{\partial r}-\frac{4}{r}\frac{\partial^2 w}{\partial r^2}\right),$$
$$\tau^{(1)}_{zzz} = \frac{2\mu(z)l_1^2}{5}\left(\frac{\partial^2 w}{\partial r^2}+\frac{1}{r}\frac{\partial w}{\partial r}\right)$$
$$\tau^{(1)}_{z\theta\theta} = \tau^{(1)}_{\theta\theta z} = \tau^{(1)}_{\theta z\theta} = \frac{2\mu(z)l_1^2}{15}\left(\frac{\partial^2 w}{\partial r^2}-\frac{4}{r}\frac{\partial w}{\partial r}\right)$$
$$\tau^{(1)}_{rzz} = \tau^{(1)}_{zzr} = \tau^{(1)}_{zrz} = \frac{2z\mu(z)l_1^2}{15}\left(3\frac{\partial^3 w}{\partial r^3}-\frac{1}{r^2}\frac{\partial w}{\partial r}+\frac{1}{r}\frac{\partial^2 w}{\partial r^2}\right),$$
$$\varepsilon_{rr} = -z\frac{\partial^2 w}{\partial r^2},\quad \varepsilon_{\theta\theta} = -\frac{z}{r}\frac{\partial w}{\partial r}$$
$$\sigma_{rr} = \frac{E(z)}{(1-\upsilon(z)^2)}\left(-z\left(\frac{\partial^2 w}{\partial r^2}+\frac{\upsilon(z)}{r}\frac{\partial w}{\partial r}\right)-\alpha(z)(1+\upsilon(z))T\right)$$
$$\sigma_{\theta\theta} = \frac{E(z)}{(1-\upsilon(z)^2)}\left(-z\left(\frac{1}{r}\frac{\partial w}{\partial r}+\upsilon(z)\frac{\partial^2 w}{\partial r^2}\right)-\alpha(z)(1+\upsilon(z))T\right) \qquad (32)$$

Couple moments, bending moments, higher order resultants force and moments:

$$M_{rr} = \int_{-h/2}^{h/2}\frac{E(z)z}{(1-\upsilon^2)}\begin{pmatrix}-z\left(\dfrac{\partial^2 w}{\partial r^2}+\dfrac{\upsilon}{r}\dfrac{\partial w}{\partial r}\right)\\ -\alpha(z)(1+\upsilon)T\end{pmatrix}dz,$$
$$M_{\theta\theta} = \int_{-h/2}^{h/2}\frac{E(z)z}{(1-\upsilon^2)}\begin{pmatrix}-z\left(\dfrac{1}{r}\dfrac{\partial w}{\partial r}+\upsilon\dfrac{\partial^2 w}{\partial r^2}\right)\\ -\alpha(z)(1+\upsilon)T\end{pmatrix}dz,$$
$$N_{rr} = \int_{-h/2}^{h/2}\frac{E(z)}{(1-\upsilon^2)}\begin{pmatrix}-z\left(\dfrac{\partial^2 w}{\partial r^2}+\dfrac{\upsilon}{r}\dfrac{\partial w}{\partial r}\right)\\ -\alpha(z)(1+\upsilon)T\end{pmatrix}dz,$$
$$N_{\theta\theta} = \int_{-h/2}^{h/2}\frac{E(z)}{(1-\upsilon^2)}\begin{pmatrix}-z\left(\dfrac{1}{r}\dfrac{\partial w}{\partial r}+\upsilon\dfrac{\partial^2 w}{\partial r^2}\right)\\ -\alpha(z)(1+\upsilon)T\end{pmatrix}dz,$$
$$Y_{r\theta} = \int_{-h/2}^{h/2}\mu(z)l_2^2\left(-\frac{\partial^2 w}{\partial r^2}+\frac{1}{r}\frac{\partial w}{\partial r}\right)dz$$
$$\mathrm{P}_z = -\int_{-h/2}^{h/2}2\mu(z)l_0^2\left(\frac{\partial^2 w}{\partial r^2}+\frac{1}{r}\frac{\partial w}{\partial r}\right)dz \qquad (33)$$